Semi-Interpenetrating Polymer Network Hydrogels Based on Aspen Hemicellulose and Chitosan: Effect of Crosslinking Sequence on Hydrogel Properties

Muzaffer Ahmet Karaaslan,[1] Mandla A. Tshabalala,[2] Gisela Buschle-Diller[1]

[1]*Department of Polymer and Fiber Engineering, Auburn University, Auburn, Alabama 36849-5327*
[2]*USDA Forest Products Laboratory, Madison, Wisconsin 53726*

Received 12 July 2010; accepted 13 June 2011
DOI 10.1002/app.35075
Published online 12 October 2011 in Wiley Online Library (wileyonlinelibrary.com).

ABSTRACT: Semi-interpenetrating network hydrogel films were prepared using hemicellulose and chemically crosslinked chitosan. Hemicellulose was extracted from aspen by using a novel alkaline treatment and characterized by HPSEC, and consisted of a mixture of high and low molecular weight polymeric fractions. HPLC analysis of the acid hydrolysate of the hemicellulose showed that its major constituent sugar was xylose. X-ray analysis showed that the relative crystallinity of hydrogels increased with increasing hemicellulose content up to 31.3%. Strong intermolecular interactions between chitosan and hemicellulose were evidenced by FT-IR analysis. Quantitative analysis of free amino groups showed that hemicellulose could interrupt the chemical crosslinking of chitosan macromolecules. Mechanical testing and swelling experiments were used to define the effective network crosslink density and average molecular weight between crosslinks. Swelling ratios increased with increasing hemicellulose content and mainly consisted of H-bonded bound water. Results revealed that by altering the hydrogel preparation steps and hemicellulose content, crosslink density and swelling behavior of semi-IPN hydrogels could be controlled without deteriorating their mechanical properties. © 2011 Wiley Periodicals, Inc. J Appl Polym Sci 124: 1168–1177, 2012

Key words: hemicellulose; hydrogel; film; semi-interpenetrating; chitosan

INTRODUCTION

Hemicelluloses are a class of hetero-polysaccharides present in the cell wall of wood and annual plants together with cellulose and lignin. They are considered to be the second most abundant polysaccharide in nature, representing about 20%–35% of lignocellulosic biomass.[1] Increasing interest in materials derived from renewable resources has rekindled intensive research into new applications for hemicelluloses. Due to their inherent hydrophilicity, low toxicity, biodegradability, and biocompatibility, the formation of hydrogels is a potential area of application for hemicelluloses and their derivatives.[2–4]

Hydrogels are crosslinked networks of hydrophilic polymers that are capable of retaining considerable amounts of water or biological fluids without disintegration. In addition to their high liquid uptake, stimuli-responsive swelling capabilities and biocompatibility are some of the features that render them suitable for biological and biomedical applications.[5–7] However, most hydrogels show relatively low mechanical stability. A considerable amount of effort is focused on improving the chemical and/or physical crosslinks between the macromolecular chains without impairing their sorption capabilities.[8–10] The formation of semi-interpenetrating networks (semi-IPNs)—blending two polymers with one being crosslinked in the presence of the other (not crosslinked) polymer—is a possible strategy that has been widely studied.[11–14] In addition to chemical crosslinks, additional interactions including hydrogen bonds, crystallites, ionic, and hydrophobic interactions may contribute to the characteristics of the resulting hydrogel.[15–17]

In our previous study, we synthesized semi-interpenetrating network hydrogel films from aspen hemicellulose and chitosan and investigated their potential applications as pH-sensitive controlled drug delivery vehicles.[18] The mechanical stability of hydrogels was predominantly influenced by covalent crosslinks rather than crystallites introduced through hemicellulose. Aspen hemicelluloses had been freeze-dried and contained some acetyl groups. As discussed by Berger et al.,[15] strong intermolecular interactions between chitosan and an additional hydrophilic polymer, hemicellulose in our case, was suggested to be the interfering factor for covalent crosslinking of chitosan chains and resulted in the reduction of overall crosslink density, lower modulus, and strength. For the current study, extraction

Correspondence to: G. Buschle-Diller (buschgi@auburn.edu).

of hemicellulose from fresh aspen chips was performed under conditions that resulted in substitution of the acetyl groups with hydroxyl groups, which in turn enabled additional hydrogen bonding within the hydrogel.

The aim of the present work was to control the crosslink density and the mechanical properties of hemicellulose/chitosan semi-IPN hydrogels by changing the crosslinking sequence. It has been hypothesized that by performing the crosslinking step before introducing hemicellulose, covalent crosslinking of chitosan would not be hindered and therefore more and/or shorter crosslinks could be formed. Furthermore, additional secondary interactions and crystalline domains introduced through hemicellulose could be favorable in terms of mechanical stability of semi-IPN hydrogels.

EXPERIMENTAL

Materials

Chitosan with 190,000–310,000 g/mol viscosity average molecular weight with 75%–85% degree of deacetylation and ninhdyrin solution (2%) were obtained from Sigma Aldrich. Glutaraldehyde, acetic acid, and other solvents and chemicals were purchased from Fisher Scientific and used as received.

Isolation of hemicelluloses

Hemicellullose, isolated from fresh aspen chips and milled by a commercial blender, was extracted by a novel alkaline extraction method, which was provided by USDA Forest Products Laboratory, Madison, WI. To remove low-molecular weight sugars from hemicellulose, the hemicellulose isolate was purified by dialysis in a Spectra/PorR dialysis membrane, MWCO: 3500. A more detailed isolation procedure has been described by Karaaslan et al.[18] The sugar content analyzed by HPLC with electrochemical detection is given in Table I.

TABLE I
Sugar Composition of Hydrolysates of Hemicellulose Fractions (%) from Fresh Aspen Chips

Component	Amount (%)
Arabinose	ND*
Galactose	0.48
Rhamnose	0.26
Glucose	0.93
Xylose	69.7
Mannose	0.29
Lignin ash	0.35
Klason Lignin	0.7
Unknowns	27.29

ND* Not detected.

Hydrogel preparation

Chitosan was dissolved in 2% v/v acetic acid aqueous solution to prepare 1% w/w chitosan solution. Hemicellulose was added to deionized water at 1% w/v and heated to 95°C for 20 min with stirring. The solution was cooled to room temperature.

To evaluate the effect of the order of sequential blending, semi-IPN hydrogels were prepared in two ways. In the first method (semi-IPN-1), chitosan and hemicellulose solutions at 70 : 30 and 30 : 70 weight ratios with a total dry matter of 1% were stirred for 8 h. For crosslinking, glutaraldehyde was added at a set ratio (3% w/w) to the total dry weight of chitosan and the mixture stirred for additional 8 h. In the second method (semi-IPN-2), glutaraldehyde reaction with chitosan was performed first, and then hemicellulose solution was added sequentially at the same weight ratios. The mixture was also stirred for 8 h. Crosslinked chitosan control samples (CS) were prepared accordingly without addition of hemicellulose.

Final solutions were cast into films in petri dishes and dried in an oven at 40°C for 24 h. The dry films were immersed in 0.1*N* sodium hydroxide solution to neutralize acetic acid residues and then washed with ethanol to remove excess NaOH. After rinsing with deionized water to remove any residual low-molecular weight compounds, including unreacted glutaraldehyde, the films were dried in an oven at 40°C for 24 h.

Hydrogel characterization

Mechanical properties

Tensile testing of the swollen hydrogel films at equilibrium was performed with an Instron Universal Tester with a 2.5 N load cell. Gauge length and crosshead speed were set to 10 mm and 2 mm/min, respectively. Samples were cut into 7×30 mm^2 strips before immersing in deionized water. In order not to damage the swollen samples during the thickness measurements, they were gently sandwiched between microscope cover slips. To prevent water loss during testing, hydrogel samples were coated with petroleum gel.[19] Mean values and 95% confidence intervals of at least ten replicates were reported.

Swelling behavior

Preweighed dry films were immersed in deionized water at room temperature for 1 h, which was previously determined to be sufficient to reach the equilibrium state. The weight of the swollen samples was measured after blotting excessive water gently with filter paper. The equilibrium swelling ratio (S) was calculated by eq. (1),

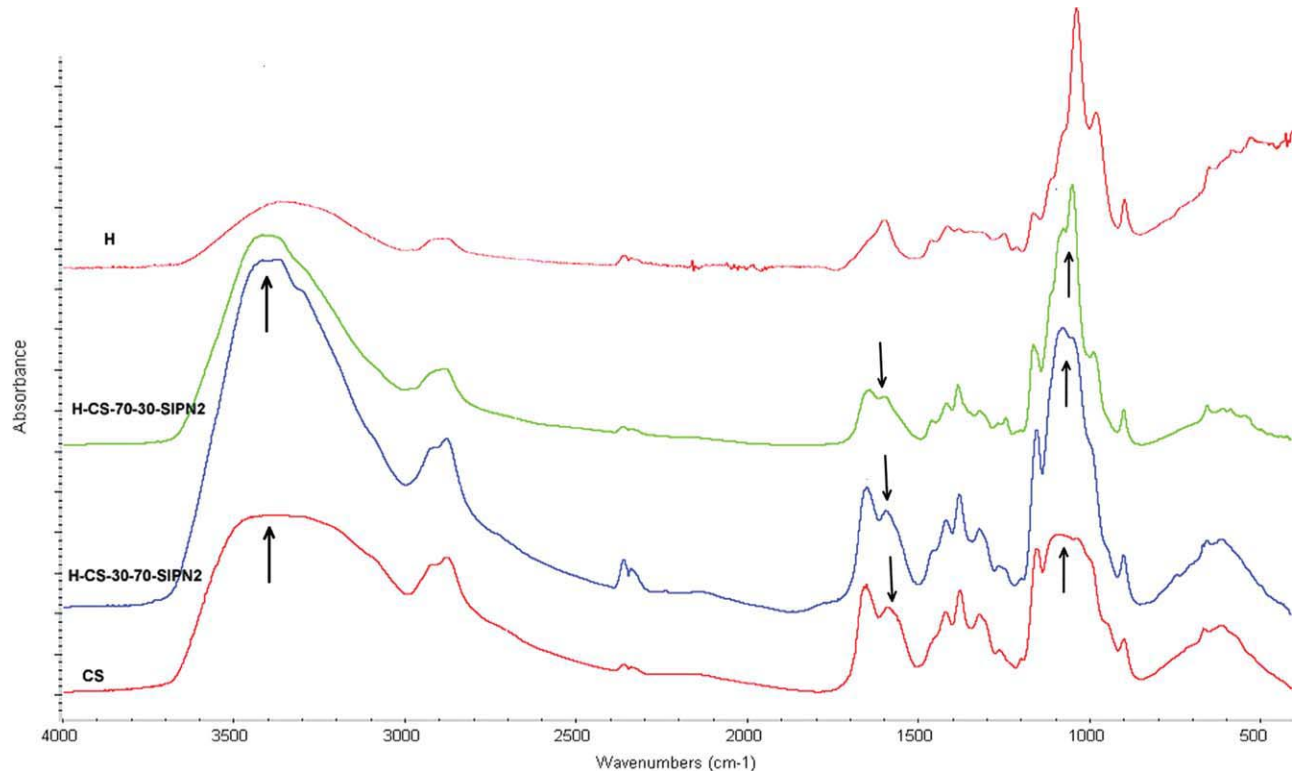

Figure 1 FT-IR spectra of semi-IPN-2 films, chitosan (CS), and hemicellulose (H) control samples. Arrows show the peak shifts observed for the NH deformation band (~ 1590 cm^{-1}) and O—H/N—H stretching band (~ 3360 cm^{-1}) and as well as more pronounced peaks (1070 and 1035 cm^{-1}). [Color figure can be viewed in the online issue, which is available at www.wileyonlinelibrary.com.]

$$S(\%) = \frac{W_S - W_d}{W_d} \times 100 \quad (1)$$

where W_S and W_d are the swollen and dry weight of samples, respectively. Equilibrium volume swelling ratio (Q_s) was determined from eq. (2):

$$Q_S = \frac{V_S}{V_d} = 1 + \frac{\rho_P}{\rho_S}(q - 1) \quad (2)$$

where V_S is volume of the swollen hydrogel, V_d is volume of the dry hydrogel, ρ_P is the density of the polymer, ρ_S is the density of deionized water, and q is the ratio of equilibrium swollen weight to dry weight (W_S/W_d). The density of semi-IPN films was determined by the floating method with carbon tetrachloride and *n*-heptane, as described by Jagadish et al.[20]

Differential scanning calorimetry (DSC, TA Instruments) was used to study the state of water in the swollen hydrogels. A piece of equilibrium swollen sample (2–4 mg) was sealed in an aluminum pan. After equilibrating for 3 min at −50°C, the sample was heated to 25°C at a rate of 5°C/min. The nonfreezing bound water and free water of the hydrogels were determined by using eq. (3),

$$W_b(\%) = S(\%) - (\Delta H_m/\Delta H_0) \times 100 \quad (3)$$

where W_b is the percentage of bound water, S (%) is the equilibrium swelling ratio, ΔH_m and ΔH_0 (334 J/g) are the melting endothermic heat of measured free water in the hydrogel and pure water, respectively.[21]

Hydrogel structural analysis

The amount of free amino groups (NH_2) in semi-IPN hydrogels was determined by ninhydrin assay according to the standard procedure. FTIR spectra of dry films were obtained with a Nicolet 6700 FT-IR spectrometer in transmission mode between 4000 and 400 cm^{-1} over 64 scans with a resolution of 4 cm^{-1}. The crystallinity of the films was analyzed by using a Rigaku Miniflex X-ray diffractometer. Cu Kα radiation at 30 kV and 15 mA with a wavelength of 1.54 Å was used, and 2θ was varied between 5° and 30° at a rate of 1° per min and a step size of 0.02°. The relative crystallinity of films was determined by the percent ratio of area under the peak at about 2θ = 18° to the total area under the peak.[22]

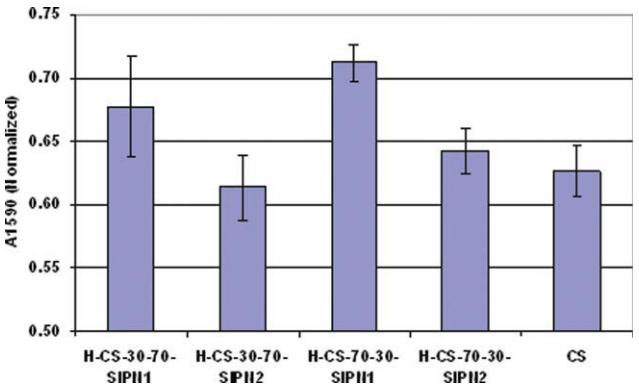

Figure 2 Comparison of the normalized N—H deformation absorbance band at 1590 cm^{-1} for semi-IPN-1 and −2 films (mean values and 95% confidence intervals reported, $n = 5$). [Color figure can be viewed in the online issue, which is available at www.wileyonlinelibrary.com.]

Surface morphology of semi-IPN films was evaluated by a Zeiss EVO50 scanning electron microscope operating with an accelerating voltage of 20 kV. Swollen films were oven-dried and sputter coated with gold prior to observation.

Thermogravimetric analysis (TGA, TA Instruments) of semi-IPN hydrogel films was carried out between 25°C and 500°C with a 20°C/min heating rate under nitrogen flow.

Semi-IPN hydrogel films, CS control sample, and hemicellulose powder in their dry state were further analyzed with DSC by two scans. In the first scan, to eliminate residual water, samples were heated from 25°C to 110°C at a rate of 20°C/min and kept at 110°C for 20 min. The second scan was performed to determine the thermal transitions and samples were heated from 25°C to 250°C at a rate of 10°C/min.

RESULTS AND DISCUSSION

Hemicellulose extraction

Sugar analysis of hemicellulose fractions (Table I), isolated for this study, yielded xylan-rich (70%) heteropolysaccharides with gluco-, galacto- mannan,- and rhamnan-residues. In our previous study,[23] NMR analysis of the hemicellulose isolate showed that the sugar residues did not carry any acetyl groups. The carboxyl group (—COOH) content was estimated by acid-base titration of hemicellulose solution and found to be 0.02–0.025 mmol/g. HPSEC results revealed a fair amount of polymeric saccharides with apparent peak molecular weights at $M_p \approx$ 401,000 and 391,000 g/mol, which is relatively high compared with other xylans reported in the literature (e.g., oat spell xylan and commercially available birchwood xylan).[24,25]

Aqueous hemicellulose solution (1% w/v) casted onto a glass plate did not produce films but brittle flakes, which might be attributed to its fairly low molecular weight and high glass transition temperature.[26] X-ray analysis showed that the hemicellulose used in this study had a crystallinity of 42.9%, which is comparable to data reported in the literature for alkaline extracted hemicelluloses.[22,26] The crystallinity of semi-IPN films with 70% and 30% hemicellulose content was determined to be 31.3% and 15.4%, respectively.

Effect of crosslinking sequence on the formation of semi-IPNs—FT-IR analysis

Figure 1 shows FT-IR spectra of semi-IPN-2 hydrogel films in comparison to crosslinked chitosan film (CS) and hemicellulose flakes (H) as the control samples. All spectra were normalized using 2880 cm^{-1}

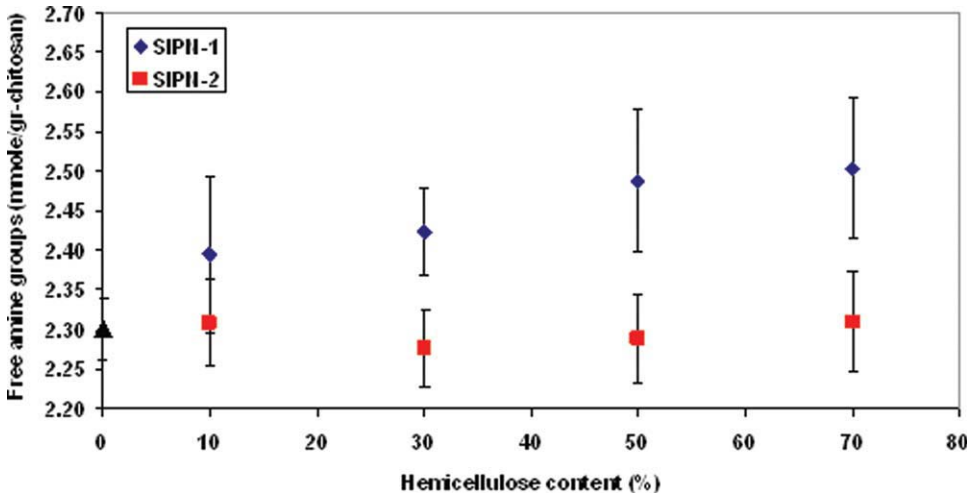

Figure 3 The amount of free amine groups determined by ninhydrin method and its dependence on hemicellulose content for semi-IPN-1 and −2 hydrogels (triangle represents the CS control sample). [Color figure can be viewed in the online issue, which is available at www.wileyonlinelibrary.com.]

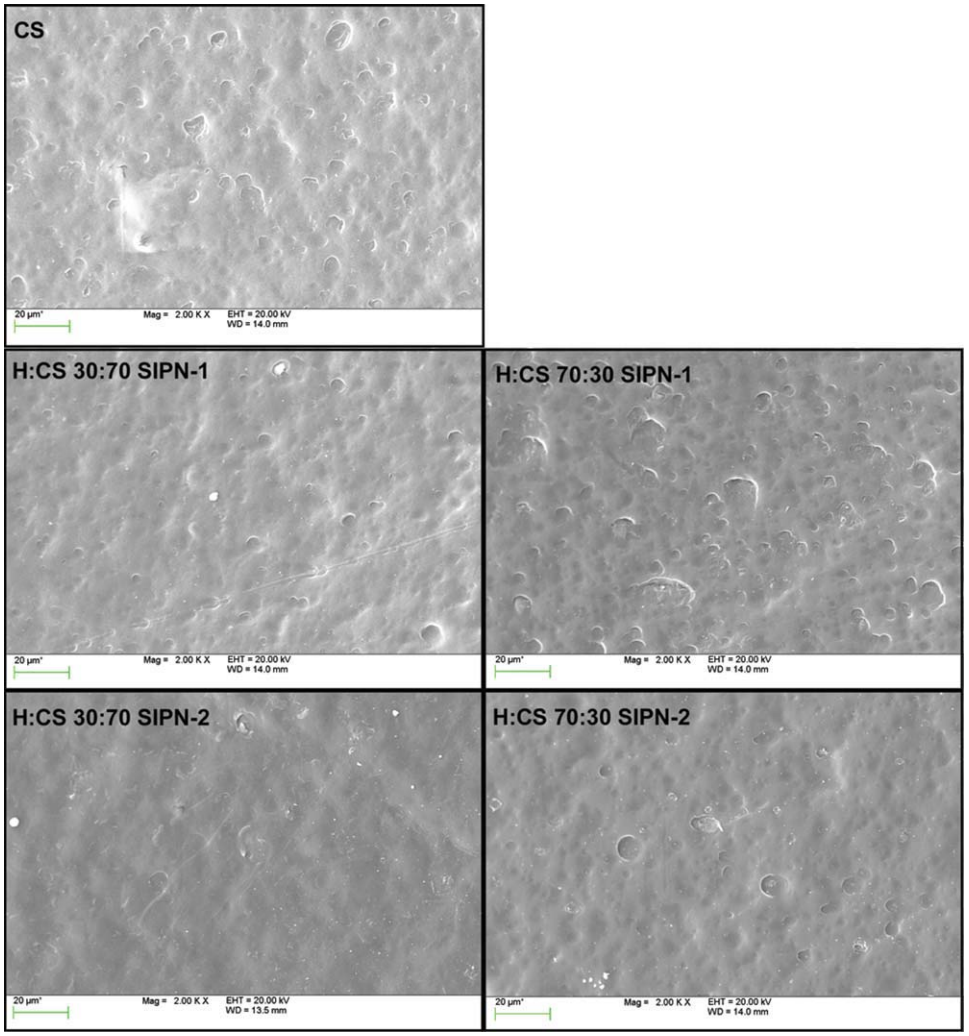

Figure 4 SEM images of the surface of semi-IPNs and the control sample (CS) at 2000× magnification. [Color figure can be viewed in the online issue, which is available at www.wileyonlinelibrary.com.]

as the reference peak as described by Kolhe and Kannan.[27] Data for semi-IPN-1 films are not shown because absorbance bands were very similar to semi-IPN-2 films.

Major absorbance bands for the CS control sample were at 1651 cm^{-1} for imide (C=N stretching) and amide I bond (C=O stretching); 1590 cm^{-1} for amide II (N—H deformation), and a broad peak at 3200–3500 cm^{-1} for N—H and O—H stretching. These bands could be seen in both semi-IPN-1 and semi-IPN-2 hydrogel films with 30% and 70% hemicellulose content. Major peaks for hemicellulose were a broad O—H stretching band at about 3400 cm^{-1}, and vibrations belong to glycosidic linkages and saccharide ring at 1070, 1035, 981, and 898 cm^{-1}. Unfortunately, these bands overlapped with chitosan peaks and were difficult to distinguish in semi-IPN films. For both semi-IPN-1 and −2 films, peak shifts were observed at the NH deformation band (from 1590 cm^{-1} to 1601 cm^{-1}) and O—H/—-H stretching band (from 3360 to 3410 cm^{-1}). In addition, absorbance bands at 1070 and 1035 cm^{-1} became more pronounced and narrower with increasing hemicellulose content. These differences in both semi-IPNs might be attributed to the strong intermolecular interactions such as H-bonding and hydrophobic attractions between hemicellulose and chitosan chains.

The quantitative FT-IR analysis (Fig. 2) did not show any significant difference between semi-IPN-1 and −2, except for the normalized N—H deformation band at 1590 cm^{-1}. This band is characteristic for amino groups attached to the chitosan backbone[28,29] and could be used to evaluate the amount of free amino groups which did not undergo a cross-linking reaction with glutaraldehyde. As shown in Figure 2, semi-IPN-2 films had lower absorbance values than those of semi-IPN-1 films for both hemicellulose compositions. The mean absorbance values for semi-IPN-2 films were relatively similar to cross-linked control CS films. This indicated that the amount of free amine groups for semi-IPN-2 and CS

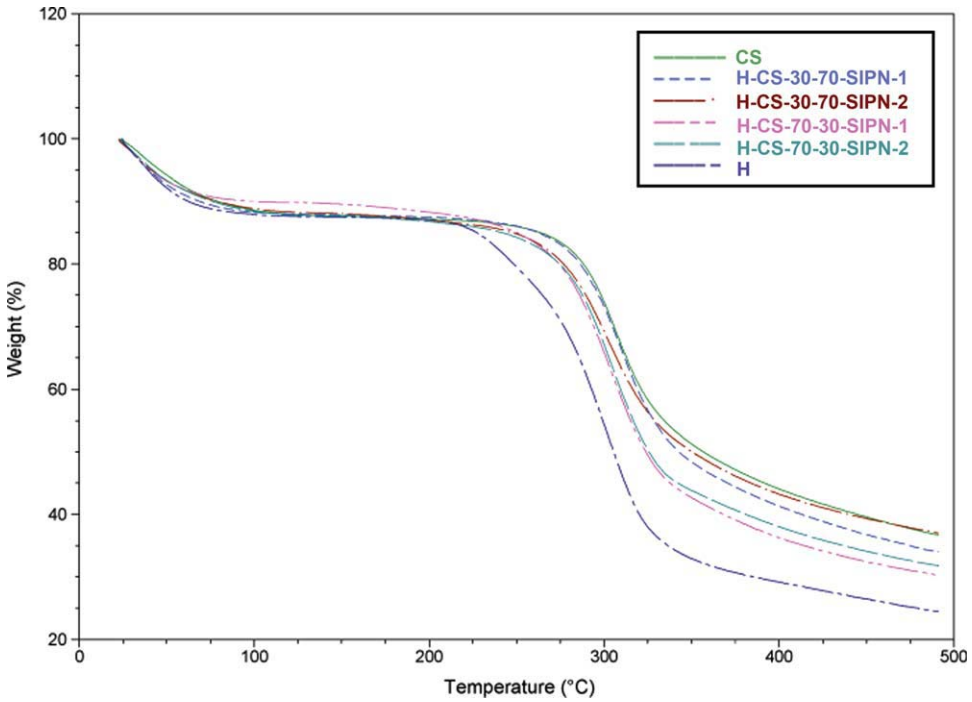

Figure 5 TGA thermograms of semi-IPN-1 and −2 films, chitosan (CS), and hemicellulose (H). [Color figure can be viewed in the online issue, which is available at www.wileyonlinelibrary.com.]

films was comparable. For both samples the amount was lower than that of semi-IPN-1 films.

The ninhydrin analysis (Fig. 3) of available amine groups showed that hemicellulose interfered in the covalent crosslinking reaction of chitosan chains with glutaraldehyde. This assay method is commonly used for quantitative determination of free amino groups in chitosan.[30,31] Figure 3 shows the average molar quantity of free amino groups ($-NH_2$) per unit chitosan weight and its dependence on hemicellulose composition in semi-IPN-1 and −2 hydrogels. Apparently, the amount of free amino groups in semi-IPN-1 hydrogels was fairly high compared to semi-IPN-2 hydrogels. Moreover, it increased slightly with increasing hemicellulose content for semi-IPN-1 hydrogels, suggesting that the interference of crosslinking reaction was also dependent on the hemicellulose content. Available amine groups for semi-IPN-2 hydrogels were at comparable level to the CS control sample and did not seem to depend on the hemicellulose content. In this case there was no obvious interference of hemicellulose on the crosslinking reaction.

Surface morphologies of semi-IPN films were examined by SEM and shown in Figure 4. The surface of semi-IPN-1 and −2 films were uniform and dense, similar to the control sample. No indication of macroscopic phase separation was observed, suggesting good miscibility between hemicellulose and chitosan because of strong intermolecular interactions. Roughness and a slightly porous texture of the surfaces may be attributed to air bubbles removed during film formation.

TGA thermograms of semi-IPN films, control sample (CS), and hemicellulose are shown in Figure 5. All samples experienced two distinct weight losses at about 100°C and about 250°C–275°C, which was because of the evaporation of water and degradation of chitosan/hemicellulose polymer chains, respectively. Hemicellulose had a lower decomposition temperature and char yield indicating low thermal stability compared with CS. This might probably be because of the presence of a portion of relatively low molecular weight hemicellulose. Thermal stability of semi-IPN-1 and −2 films was found to be in-between that of CS and hemicellulose and increased with increasing CS content.

DSC curves of CS, hemicellulose (H), and semi-IPN films are shown in Figure 6(a). In all samples, no endothermic peak of evaporating water at about 100°C has been detected. This was because of the removal of water molecules at the first DSC heating scan. In the second heating scan, no phase transition has been observed in the crosslinked chitosan (CS) control samples. This is in accordance with the fact that the glass transition temperature (T_g) of chitosan is difficult to detect with DSC since its T_g and thermal degradation temperature are close.[32] The same phenomenon has been reported for the hardwood xylan, however its T_g was estimated to be around 180°C.[26,33] In this study, DSC curve of hemicellulose showed a broad and weak transition between 163°C and 180°C and it slightly shifted to higher

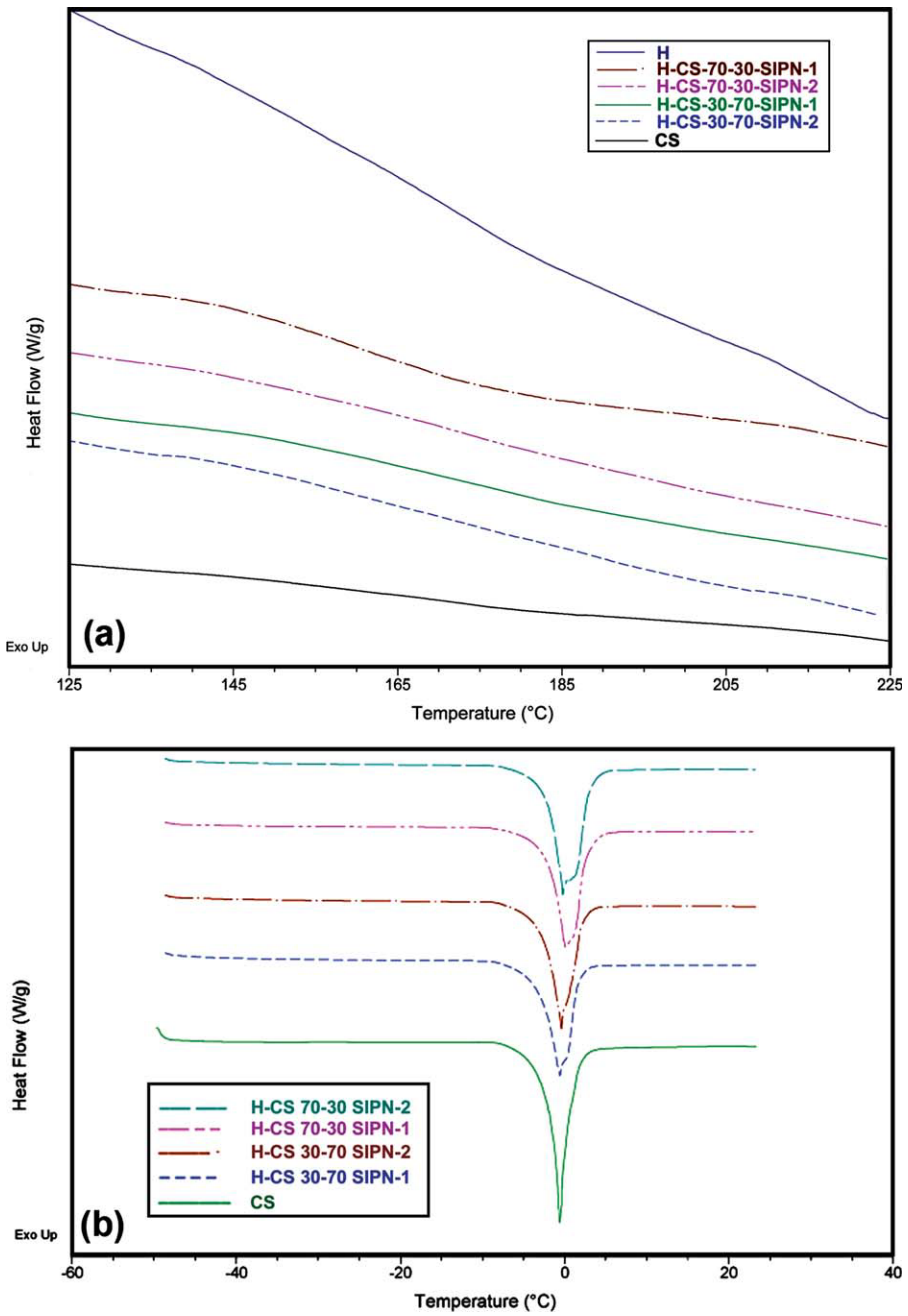

Figure 6 DSC thermograms of semi-IPN films (a) second heating scan of dry films (CS: crosslinked chitosan, H: hemicellulose powder. (b) Melting endothermic peaks of swollen films at 0°C. [Color figure can be viewed in the online issue, which is available at www.wileyonlinelibrary.com.]

temperatures as the chitosan content increased. This might be attributed to the entrapment and restricted mobility of hemicellulose chains in the semi-IPN structure as the chitosan content increased.[34,35]

Mechanical properties and network parameters

Stress–strain curves of swollen semi-IPN hydrogel films obtained from uniaxial tensile testing showed two regions with different slopes (data not shown). The slope of the curves was clearly lower for elongations below 15% than above. Thus, to more precisely estimate the elastic modulus and network parameters, Flory's statistical rubber elasticity and Mooney-Rivlin theory were used for low and high elongations, respectively.

Elastic moduli of hydrogels, G, at low elongations were determined from the slope of stress–strain curves obtained by using eq. (4),

$$\tau = G\left[\lambda - \frac{1}{\lambda^2}\right] \tag{4}$$

TABLE II
Mechanical Properties of Swollen CS and Semi-IPN Hydrogels

	G (MPa)	$G^* = 2C_1$ (MPa)	σ (MPa)	ε (%)
CS	1.65 ± 0.21	6.30 ± 1.14	1.07 ± 0.25	26.89 ± 4.10
H-CS 30–70 SIPN-1	1.63 ± 0.13	7.06 ± 0.85	1.22 ± 0.24	26.51 ± 3.21
H-CS 30–70 SIPN-2	1.74 ± 0.18	7.83 ± 0.85	1.23 ± 0.21	26.32 ± 2.72
H-CS 70–30 SIPN-1	1.02 ± 0.20	4.77 ± 0.92	0.67 ± 0.24	24.94 ± 3.90
H-CS 70–30 SIPN-2	0.87 ± 0.10	4.41 ± 0.67	0.37 ± 0.09	20.61 ± 2.40

Low elongation modulus calculated using Flory's statistical rubber elasticity theory (G, for E ≤ 15%), high elongation modulus calculated using Mooney-Rivlin constants (G^*, for E > 15%), tensile strength at break (σ) and elongation at break (E) given in averages and 95% confidence intervals brackets ($N > 10$).

where τ is the force per unit of initial cross-sectional area of swollen gel and λ is the deformation ratio (deformed length/initial length) of the network. According to Flory's statistical rubber elasticity theory, the number of effectively crosslinked chains per unit volume (ν_e, effective crosslink density) was calculated by using eq. (5),[36–38]

$$\nu_e = \frac{G}{RT\upsilon_2^{1/3}} \tag{5}$$

where ν_e is the effective crosslink density in mol/cm^3, υ_2 is the polymer volume fraction at equilibrium swollen state, R is the gas constant, and T is the temperature in Kelvin. The average molecular weight between crosslinks ($\overline{M_C}$, g/mol) was calculated by using eq. (6),

$$\overline{M_C} = \frac{1}{\nu_e \overline{\upsilon}} \tag{6}$$

where $\overline{\upsilon}$ is the specific volume of the polymer in cm^3/g.

Mooney-Rivlin theory can be expressed by the following equation;

$$\tau = 2\left(C_1 + \frac{C_2}{\lambda}\right)\left(\lambda - \frac{1}{\lambda^2}\right) \tag{7}$$

TABLE III
Effective Crosslink Density and Average Molecular Weight between Crosslinks Calculated from Elastic Modulus of Swollen Hydrogel Films

	ν_e (10^4.mol/cm^3)	ν_e^* (10^4.mol/cm^3)	$\overline{M_C}$ (g/mol)	$\overline{M_C}^*$ (g/mol)
CS	9.8	25.7	1415	627
H-CS 30–70 SIPN-1	10.2	28.8	1360	506
H-CS 30–70 SIPN-2	10.8	31.9	1286	460
H-CS 70–30 SIPN-1	6.5	20.5	2097	732
H-CS 70–30 SIPN-2	5.5	18.0	2472	810

ν_e and $\overline{M_C}$ are calculated from ε ≤ 15% and ν_e^* and $\overline{M_C}^*$ from ε > 15%.

where C_1 and C_2 are the elastic parameters. They can be obtained by plotting $\tau/(\lambda - \lambda^{-2})$ versus λ^{-1} using the linear portion of the plots.[39] These constants are independent of elongation and $G^* = 2C_1$ can be taken as an estimate of the high-elongation modulus.[40] In the present study, for ε > 15%, $G = 2C_1$ was used to estimate the modulus, the effective crosslink density [ν_e^*, eq.(8)] and the average molecular weight between the crosslinks [$\overline{M_C}^*$, from eq. (6)]. Here, ε is the percentage elongation of samples under applied stress.

$$\nu_e^* = \frac{RT}{2C_1} \tag{8}$$

The elastic modulus, tensile strength, elongation at break data, and hydrogel network parameters calculated are given in Tables II and III. Although calculated network parameters and modulus values from both sets of equations were significantly different, they followed the same trend. This showed that both theories could be applied to define the semi-IPN network structure prepared in the present study.

Samples at H–CS 30–70 ratio had been compared to those of CS. The results show that at a ratio of 30–70 H–CS, a denser network structure with shorter/more crosslinks was formed which might be

TABLE IV
Equilibrium Swelling Ratio (S), Bound Water, Free Water, and Melting Endothermic Heat (ΔH_m) of Swollen Semi-IPN and CS Hydrogels

	S (%)	Bound water (%)	Free water (%)	ΔH_m (J/g)
CS	153 ± 17	103	50	167
H-CS 30–70 SIPN-1	191 ± 20	149	42	141
H-CS 30–70 SIPN-2	181 ± 18	135	44	152
H-CS 70–30 SIPN-1	207 ± 23	160	47	155
H-CS 70–30 SIPN-2	210 ± 18	159	51	172

the main reason for enhanced modulus and strength (higher G^* values and higher tensile strength at break, higher ν_e, ν_e^* and lower $\overline{M_C}$, $\overline{M_C}^*$ compared to CS samples).

In regard to the preparation sequence of H–CS 30–70 hydrogels, semi-IPN-2 samples showed slightly higher ν_e, ν_e^* and lower $\overline{M_C}$, $\overline{M_C}^*$ (Table III), most likely because of a lower amount of free amino groups and more covalently crosslinked chains as determined with quantitative FT-IR analysis and ninhyrin assay.

Increasing the amount of hemicellulose in the hydrogels did not improve the modulus and strength values (semi-IPNs with H-CS 70–30). This might be related to a decrease in effective crosslink density and simultaneous increase in average molecular weight between crosslinks (Table III). Overall the mechanical stability was reduced as a result of a more open network structure with longer/fewer crosslinks. Mechanical properties similar to CS samples could not be maintained (Table II) regardless of the preparation sequence. H–CS 70–30 samples were fairly brittle.

Swelling behavior

It was expected that the crosslink density and the average length of the crosslinks has an effect on hydrogel swelling. The percentage equilibrium swelling ratios of semi-IPN hydrogels are listed in Table IV. With increasing hemicellulose content, swelling ratios increased compared to hydrogels made from 100% CS, indicating a higher capacity for water uptake. With the help of DSC analysis, the amount of free water and nonfreezing bound water was determined. Nonfreezing water represents water that is bound by hydrogen bonding to the polymer chains and can be calculated by the difference between the total amount of water inside the gel and free water. Free water includes freezing free water and freezing bound water indicated by the endothermic peak of the DSC curve at 0°C, as shown in Figure 6(b).[21]

As shown in Table IV, the main percentage of water inside the swollen hydrogels was bound water. The amount of bound water was higher in all semi-IPNs and increased with increasing hemicellulose content compared to CS samples. The results clearly demonstrated the impact of longer crosslinks at H–CS 70–30 ratios with higher potential for interaction of water molecules with polymer chains.

CONCLUSIONS

Alkaline extracted aspen hemicellulose was successfully used to prepare semi-interpenetrating (semi-IPN) hydrogel films with chitosan. The apparent peak molecular weight (M_p) of the hemicellulose was fairly high. Crystallinity of hydrogel films increased with increasing hemicellulose content. Hemicellulose is capable of disturbing the covalent crosslinking reaction of chitosan chains during semi-IPN formation. This effect could be controlled by altering hydrogel preparation steps. Increasing hemicellulose content increased the amount of H-bonded bound water and enhanced the overall swelling capacity of hydrogel films. This study showed that by altering the sequence of the hydrogel preparation steps and the hemicellulose content, crosslink density and swelling properties of semi-IPN hydrogels can be controlled without negatively impacting their mechanical properties.

The authors are grateful for the support of the Wood Education and Resource Center (WERC).

References

1. Timell, T. E. Wood Sci Technol 1967, l, 45.
2. Coviello, T.; Matricardi, P.; Marianecci, C.; Alhaique, F. J Controlled Release 2007, 119, 5.
3. Ebringerova, A. Macromol Symp 2006, 232, 1.
4. Xinming, L.; Xuejun, P. J Biobased Mater Bioenergy 2010, 4, 289.
5. Peppas, N. A.; Hilt, J. Z.; Khademhosseini, A.; Langer, R. Adv Mater 2006, 18, 1345.
6. Slaughter, B. V.; Khurshid, S. S.; Fisher, O. Z.; Khademhosseini, A.; Peppas, N. A. Adv Mater 2009, 21, 1.
7. Hoare, T. R.; Kohane, D. S. Polymer 1993, 2008, 49.
8. Schexnailder, P.; Schmidt, G. Colloid Polym Sci 2009, 287, 1.
9. Tanaka, Y.; Gong, J. P.; Osada, Y. Prog Polym Sci 2005, 30, 1.
10. Myung, D.; Waters, D.; Wiseman, M.; Duhamel, P. E.; Noolandi, J.; Ta, C. N.; Frank, C. W. Polym Adv Technol 2008, 19, 647.
11. Liu, C.; Chena, Y.; Chena, J. Carbohydr Polym 2010, 79, 500.
12. Jin, S.; Liu, M.; Zhang, F.; Chen, S.; Niu, A. Polymer 2006, 47, 1526.
13. Lu, Y.; Zhang, L. Polymer 2002, 43, 3979.
14. Zhao, Y.; Kang, J.; Tan, T. W. Polymer 2006, 47, 7702.
15. Berger, J.; Reist, M.; Mayer, J. M.; Felt, O.; Gurny R. Eur J Pharm Biopharm 2004, 57, 19.
16. Hoffman, A. S. Adv Drug Delivery Rev 2002, 43, 3.
17. Hassan, C. M.; Peppas, N. A. Macromolecules 2000, 33, 2472.
18. Karaaslan, M. A.; Tshabalala, M.; Buschle-Diller, G. Bioresources 2010, 5, 1036.
19. Anseth, K. S.; Bowman, C. N.; Bannon-Peppas, L. Biomaterials 1996, 17, 1647.
20. Jagadish, R. S.; Raj, B.; Parameswara, P.; Somashekar, R. Polym Int 2009, 59, 931.
21. Ostrowska-Czubenko, J.; Gierszewska-Druzynska, M. Carbohydr Polym 2009, 77, 590.
22. Gabrielii, I.; Gatenholm, P.; Glasser, W. G.; Jain, R. K.; Kenne, L. Carbohydr Polym 2000, 43, 367.
23. Karaaslan, M. A.; Tshabalala, M. A.; Yelle, D. J.; Buschle-Diller, G. Carbohydr Polym, to appear.
24. Henriksson, A.; Gatenholm, P. Holzforschung 2001, 55, 494.
25. Kabel, M. A.; Bornea, H.; Vincken, J. P.; Voragen, A. G. J.; Schols, H. A. Carbohydr Polym 2007, 69, 94.
26. Gröndahl, M.; Eriksson, L.; Gatenholm P. Biomacromolecules 2004, 5, 1528.

27. Kolhe, P.; Kannan, R. M. Biomacromolecules 2003, 4, 173.
28. Qu, X.; Wirsen, A.; Albertsson, A. C. Polymer 2000, 41, 4841.
29. Osman, Z.; Arof, A. K. Electrochim Acta 2003, 48, 993.
30. Curotto, E.; Aros, F. Anal Biochem 1993, 211, 240.
31. Mi, F. L.; Tan, Y. C.; Liang H. C.; Huang R. N.; Sung H. W. J Biomater Sci Polym Ed 2001, 12, 835.
32. Neto, C.G.T.; Giacometti, J. A.; Job, A. E.; Ferreira, F. C.; Fonseca, J. L. C.; Pereira, M. R. Carbohydr Polym 2005, 62, 97.
33. Irvine, G. M. Tappi 1984, 67, 118.
34. Rodkate, N.; Wichai, U.; Boontha, B.; Rutnakornpituk, M. Carbohydr Polym 2010, 81, 617.
35. Kim, S. J.; Park, S. J.; Shin, M. S.; Lee, Y. H.; Kim, N. G.; Kim, S. I. J Appl Polym Sci 2002, 85, 1956.
36. Yui, N. Supramolecular Design for Biological Applications; CRC Press: Boca Raton, FL, 2002.
37. Ma, P. X.; Elisseeff, J. H. Scaffolding in Tissue Engineering; CRC Press: Boca Raton, FL, 2005.
38. Lou, X.; Coppenhagen, C. Polym Int 2001, 50, 319.
39. Jiang, G.; Liu, C.; Liu, X.; Chen, Q.; Zhang, G.; Yang, M.; Liu, F. Polymer 2010, 51, 1507.
40. Mark, J. E.; Erman, B. Rubberlike Elasticity: A Molecular Primer; Wiley, New York, 1988.